PTEP

Prog. Theor. Exp. Phys. **2020**, 093B06 (6 pages)
DOI: 10.1093/ptep/ptaa099

Electroweak fermion triangle loop contributions to the muon anomalous magnetic moment revisited

Ken Sasaki*

Department of Physics, Faculty of Engineering, Yokohama National University, Yokohama 240-8501, Japan
*E-mail: sasaki@ynu.ac.jp

Received May 22, 2020; Revised June 20, 2020; Accepted June 21, 2020; Published September 10, 2020

The contribution to the muon anomalous magnetic moment from the fermion triangle loop diagrams connected to the muon line by a photon and a Z boson is re-analyzed in both the unitary gauge and the 't Hooft–Feynman gauge. With use of the anomalous axial-vector Ward identity, it is shown that the calculation in the unitary gauge exactly coincides with the one in the 't Hooft–Feynman gauge. The part which arises from the ordinary axial-vector Ward identity corresponds to the contribution of the neutral Goldstone boson. For the top-quark contribution, the one-parameter integral form is obtained up to the order of m_μ^2/m_Z^2. The results are compared with those obtained by the asymptotic expansion method.

Subject Index B50, B57

A discrepancy of 3.3σ still remains between experiment and the standard model (SM) prediction for the muon anomalous magnetic moment $a_\mu \equiv (g_\mu - 2)/2$ [1]. The calculations of two-loop contributions to a_μ due to the electroweak interactions of the SM were completed quite some time ago [2–5] and recently the numerically evaluated results of full two-loop electroweak corrections were presented [6]. For more references, see Ref. [1].

Two-loop electroweak corrections are relatively large and reduce the one-loop contribution $a_\mu^{\rm EW}(1\text{ loop})$ by about 21% [1]. They are expressed as the form

$$a_\mu^{\rm EW}(2\text{ loop}) = \frac{5}{3}\frac{G_\mu m_\mu^2}{8\sqrt{2}\pi^2}\sum_i C_i \frac{\alpha}{\pi} \ . \qquad (1)$$

A thorough study of the two-loop electroweak contributions to $a_\mu^{\rm EW}$ was made in Refs.[2,3], where the asymptotic expansion method was employed and the 't Hooft–Feynman gauge was used. Then in Ref. [7], for a concrete illustration of the asymptotic expansion method, Czarnecki and Marciano, coauthors of Refs.[2,3], showed in detail the calculation of the diagrams with top quark triangle loops connected to the muon line by a photon and a Z boson. The relevant Feynman diagrams are given in Fig. 1, where the top quark is replaced with a charged fermion f. In the case of f = top quark, there appear two large ratios of masses, m_t^2/m_Z^2 and m_Z^2/m_μ^2, which provides a good example to study the power of the asymptotic expansion method.

Study of a specific subset of the two-loop electroweak contributions shown in Fig. 1 is also interesting due to the fact that its fermionic triangle loop subdiagrams have the Adler–Bell–Jackiw *VVA* anomaly. The analysis of this subset of diagrams was first made by Kukhto *et al.* [4] (KKSS). They used a simplified version of the $Z\gamma\gamma$ vertex function by Adler [8] and Rosenberg [9] for the

Funded by SCOAP[3]

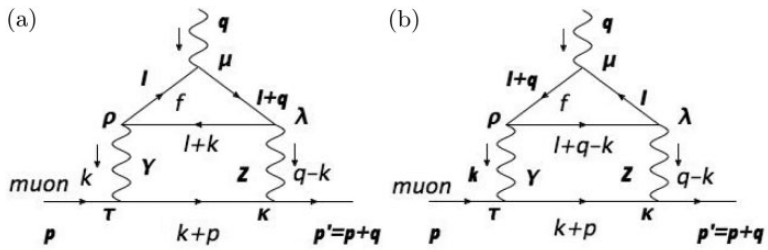

Fig. 1. Diagrams with fermion triangle loops connected to the muon line by a photon and a Z boson. The diagrams with a photon and a Z-boson interchanged should be added.

fermionic triangle subdiagrams and found that the loop contributions of leptons, i.e., e, μ and τ, were enhanced by large logarithms of the form $\ln(m_Z/m_\mu)$ or $\ln(m_Z/m_\tau)$. Then followed the studies of quark loop contributions [2,5].

In Ref. [7], the result by the asymptotic expansion method for the contributions of the top quark loop diagrams in Fig. 1 is made up of ΔC_Z and ΔC_G, which are given in Eqs. (9) and (10), respectively, of the paper and are written in terms of the two ratios, m_t^2/m_Z^2 and m_Z^2/m_μ^2. The calculation was made in the 't Hooft–Feynman gauge and ΔC_G is the contribution generated from the neutral Goldstone boson. If the integral representations for ΔC_Z and ΔC_G are obtained, they are very useful for confirming the validity of the asymptotic expansion method. It is also interesting to see what happens to ΔC_G when the diagrams are calculated in a different gauge, e.g. in the unitary gauge. These are motivations for reanalyzing the contributions to a_μ from the fermion triangle loop diagrams shown in Fig. 1.

Actually the top quark (more generally, a charged fermion) triangle loop contributions can be calculated exactly, the results of which in the unitary gauge were already given in Eqs. (13)–(15) of Ref. [5], in the form of rather complex parametric representation with five Feynman parameters. In this paper I re-examine the contributions to a_μ from the fermion triangle loop diagrams depicted in Fig. 1 in both the unitary gauge and the 't Hooft–Feynman gauge, and show that, with use of the anomalous axial-vector Ward identity, the calculation in the unitary gauge *exactly coincides with* the one in the 't Hooft–Feynman gauge. The part which arises from the ordinary axial-vector Ward identity corresponds to the contribution of the neutral Goldstone boson. Then, for the top-quark contribution, the one-parameter integral form is obtained up to the order of m_μ^2/m_Z^2. The results are compared with those obtained by the asymptotic expansion method.

The muon state before and after the interaction with a photon field with momentum q satisfies the following on-shell conditions:

$$\overline{u}(p+q)(\not{p}+\not{q}) = \overline{u}(p+q)m_\mu, \qquad \not{p}u(p) = m_\mu u(p), \tag{2}$$

where m_μ is a muon mass. In the following calculation we put $q^2 = 0$ and then the above on-shell conditions lead to $p \cdot q = 0$. It is well-known that the contributions of VVV terms in the fermionic triangle subdiagrams in Fig. 1(a) and (b) mutually cancel by virtue of Furry's theorem while the VVA terms have the Adler–Bell–Jackiw anomaly. Then we use the $Z\gamma\gamma$ vertex function derived by Adler [8] and Rosenberg [9] for the fermionic triangle subdiagrams, which reads in terms of the momenta shown in Fig. 1 as

$$R^{\mu\rho\lambda}(q,-k,k-q)=\frac{1}{\pi^2}\int_0^1 dx\int_0^{1-x}dy\Big[m_f^2-x(1-x)k^2+2xyk\cdot q\Big]^{-1}$$
$$\times\Bigg\{\Big[x(1-x)k^2-xy(k\cdot q)\Big]\epsilon^{\lambda\mu\rho q}-xy(k\cdot q)\epsilon^{\lambda\mu\rho k}+xy\,q^\rho\epsilon^{\lambda\mu kq}$$
$$-x(1-x)k^\rho\epsilon^{\lambda\mu kq}-y(1-y)q^\mu\epsilon^{\lambda\rho kq}+xy\,k^\mu\epsilon^{\lambda\rho kq}\Bigg\},\qquad(3)$$

where m_f is a fermion mass in the loop and $\epsilon^{\lambda\mu\rho q}=\epsilon^{\lambda\mu\rho\alpha}q_\alpha$, etc. The convention $\epsilon^{0123}=-\epsilon_{0123}=1$ is used, which agrees with Peskin and Schroeder [10,11] and not with Adler and Rosenberg [8,9] nor with KKSS [4]. Note that the above expression is the full-version of the $Z\gamma\gamma$ vertex function with $q^2=0$. In Ref. [4], KKSS used a simplified version of the $Z\gamma\gamma$ vertex function obtained from the full-version (3) by keeping, in the numerator, only the terms linear in the external photon momenta q and discarding the $k\cdot q$ term in the denominator. The full version $R^{\mu\rho\lambda}(q,-k,k-q)$ satisfies the electromagnetic current conservation, $q_\mu R^{\mu\rho\lambda}(q,-k,k-q)=0$ and $k_\rho R^{\mu\rho\lambda}(q,-k,k-q)=0$, and the anomalous axial-vector Ward identity

$$(k-q)_\lambda R^{\mu\rho\lambda}(q,-k,k-q)=-\frac{1}{2\pi^2}\epsilon^{\mu\rho kq}$$
$$+\frac{m_f^2}{\pi^2}\int_0^1 dx\int_0^{1-x}dy\left[m_t^2-x(1-x)k^2+2xyk\cdot q\right]^{-1}\epsilon^{\mu\rho kq}.\qquad(4)$$

The first term is the Adler–Bell–Jackiw *VVA* anomaly and is independent of the fermion mass m_f in the loop, while the second term corresponds to the ordinary axial-vector Ward identity and is proportional to m_f^2.

The calculation of the lower-loop in Fig. 1 is performed by using the Z-boson propagator in the unitary gauge,

$$\frac{-i}{(k-q)^2-m_Z^2}\left[g_{\lambda\kappa}-\frac{(k-q)_\lambda(k-q)_\kappa}{m_Z^2}\right].\qquad(5)$$

The contraction of $(k-q)_\lambda$ and the $Z\gamma\gamma$ vertex function gives the anomalous axial-vector Ward identity in Eq. (4). The anomaly term generates a divergence in the loop integral. However, it does not depend on the fermion and thus, in the SM, the contributions of the anomaly terms cancel out when all the fermions in each generation are included [5]. Hence in the following we omit the anomaly term. The calculation proceeds by making full use of an identity

$$i\epsilon_{\mu\rho\nu\lambda}\gamma^\lambda\gamma_5=\gamma_\mu\gamma_\rho\gamma_\nu-g_{\mu\rho}\gamma_\nu-g_{\rho\nu}\gamma_\mu+g_{\mu\nu}\gamma_\rho\,,\qquad(6)$$

and the on-shell conditions (2). Discarding the terms with γ_μ and picking only those with p_μ and q_μ, the remaining terms are found to be proportional to $(2p+q)_\mu$. Then the y-integration and the symmetrization in the x variable, i.e., $f(x)\to[f(x)+f(1-x)]/2$, are made.

Finally, the following expressions are obtained for the triangle loop contribution of a fermion f in rather compact integral form with four Feynman parameters,

$$C_{\gamma Z}(f)=N_c^fQ_f^2I_{3f}\frac{12}{5}\left\{A_{\gamma Z}(f)-\lambda_fB_{\gamma Z}(f)\right\},\qquad(7)$$

where

$$A_{\gamma Z}(f) = \int_0^1 dx \int_0^1 dz_4 \int_0^{1-z_4} dz_3 \int_0^{1-z_4-z_3} dz_2 \times \left\{ \frac{a(2+3z_4)}{a\kappa z_4^2 + az_2 + \lambda_f z_3} - \kappa \frac{a^2 z_4^3}{[a\kappa z_4^2 + az_2 + \lambda_f z_3]^2} \right\}, \tag{8}$$

$$B_{\gamma Z}(f) = \int_0^1 dx \int_0^1 dz_4 \int_0^{1-z_4} dz_3 \int_0^{1-z_4-z_3} dz_2 \times \left\{ \frac{1+3z_4}{a\kappa z_4^2 + az_2 + \lambda_f z_3} - \kappa \frac{a z_4^3}{[a\kappa z_4^2 + az_2 + \lambda_f z_3]^2} \right\}, \tag{9}$$

with $a \equiv x(1-x)$, $\lambda_f \equiv m_f^2/m_Z^2$ and $\kappa \equiv m_\mu^2/m_Z^2$; N_c^f, Q_f and I_{3f} are the color factor, the electric charge and the third component of weak isospin of the fermion f, respectively, with $N_c^f = 3(1)$ for quarks (leptons). These are exact results, and $A_{\gamma Z}(\lambda_f, \kappa)$ and $B_{\gamma Z}(\lambda_f, \kappa)$ are equivalent to $\mathcal{F}[m_f^2/m_\mu^2, M_Z^2/m_\mu^2]$ in Eq. (14) and $\mathcal{G}[m_f^2/m_\mu^2, M_Z^2/m_\mu^2]$ in Eq. (15) of Ref. [5], respectively. Having the expressions given in Eqs. (8) and (9), it is easy to perform further integrations with respect to the Feynman parameters z_2, z_3 and z_4. The term $A_{\gamma Z}(f)$ comes from the $g_{\lambda\kappa}$ part of the Z-boson propagator (5). On the other hand, the $B_{\gamma Z}(f)$ term arises from the ordinary axial-vector Ward identity, and thus is multiplied by the factor λ_f in Eq. (7). Due to this factor, $B_{\gamma Z}(f)$ is only relevant for the case f = top quark [5]. It is interesting to note that the expression of $A_{\gamma Z}(f)$ turns out to be the same as the one given by KKSS in Eq. (4.10) of Ref. [4], which was derived by using the simplified version of the $Z\gamma\gamma$ vertex function.

Now consider the calculation of the same diagrams in Fig. 1 in the 't Hooft–Feynman gauge. The Z-boson propagator in the 't Hooft–Feynman gauge is given by

$$\frac{-i}{(k-q)^2 - m_Z^2} g_{\lambda\kappa} , \tag{10}$$

which is the same form as the $g_{\lambda\kappa}$ part of the Z-boson propagator in the unitary gauge in Eq. (5). Hence the contribution generated from the Z-boson propagator in the 't Hooft–Feynman gauge is expressed as $A_{\gamma Z}(f)$ in Eq. (8). In addition, we need to consider the contribution generated from the neutral Goldstone boson G^0. The relevant diagrams are obtained from Fig. 1 (a) and (b) with replacement of the Z-boson propagator by that of G^0. Also, the axial-vector couplings of the Z-boson are replaced by the pseudo-scalar couplings of G^0 to the fermion in the loop and the muon. The loop-integral of the fermionic triangle subdiagrams in Fig. 1 (a) and (b) where the axial-vector vertex $\gamma^\lambda\gamma_5$ is replaced by the pseudo-scalar vertex $m_f\gamma_5$ gives

$$\frac{m_f^2}{2\pi^2} \int_0^1 dx \int_0^{1-x} dy \Big[m_t^2 - x(1-x)k^2 + 2xyk\cdot q \Big]^{-1} \epsilon^{\mu\rho kq} , \tag{11}$$

which is just one half of the second term of Eq. (4) (an ordinary axial-vector Ward identity). Now attaching the pseudo-scalar vertex $m_\mu\gamma_5$ to the muon line, the lower-loop integral is made and the following exact result is obtained for the contribution generated from the neutral Goldstone boson G^0:

$$C_{\gamma G^0}(f) = N_c^f Q_f^2 I_{3f} \frac{12}{5} (-\lambda_f) B_{\gamma G^0}(f) , \tag{12}$$

where

$$B_{\gamma G^0}(f) = \int_0^1 dx \int_0^1 dz_4 \int_0^{1-z_4} dz_3 \int_0^{1-z_4-z_3} dz_2 \times \left\{ \frac{2}{a\kappa z_4^2 + az_2 + \lambda_f z_3} - \kappa \frac{2az_4^2}{[a\kappa z_4^2 + az_2 + \lambda_f z_3]^2} \right\} . \quad (13)$$

The expressions of $B_{\gamma Z}(f)$ and $B_{\gamma G^0}(f)$ look different at first glance but actually are equivalent. Take the difference and we see that it vanishes after the integration with respect to the variables z_2, z_3 and z_4. Now it is clear that the calculation in the unitary gauge *exactly coincides with* the one in the 't Hooft–Feynman gauge. The part which arises from the ordinary axial-vector Ward identity in the unitary gauge corresponds to the contribution of the neutral Goldstone boson.

For the case $m_f^2 \gg m_\mu^2$, the integrations of $A_{\gamma Z}(f)$ and $B_{\gamma Z}(f)(= B_{\gamma G^0}(f))$ with respect to the variables z_2, z_3 and z_4 are easily made up to $\mathcal{O}(\kappa)$. The results are

$$A_{\gamma Z}(f) = \widetilde{A}_{\gamma Z}(f) + \frac{\kappa}{\lambda_f} \int_0^1 dx\, a \left\{ \frac{5}{3} \frac{a}{a-\lambda_f} \log \frac{a}{\lambda_f} + \frac{17}{18} + \frac{5}{3} \log \kappa \right\} + \mathcal{O}(\kappa^2), \quad (14)$$

$$B_{\gamma Z}(f) = \widetilde{B}_{\gamma Z}(f) + \frac{\kappa}{\lambda_f} \int_0^1 dx \left\{ \frac{4}{3} \frac{a}{a-\lambda_f} \log \frac{a}{\lambda_f} + \frac{8}{9} + \frac{4}{3} \log \kappa \right\} + \mathcal{O}(\kappa^2), \quad (15)$$

where

$$\widetilde{A}_{\gamma Z}(f) = \frac{3}{2} \int_0^1 dx \frac{a}{a-\lambda_f} \log \frac{a}{\lambda_f} , \qquad \widetilde{B}_{\gamma Z}(f) = \int_0^1 dx \frac{1}{a-\lambda_f} \log \frac{a}{\lambda_f} . \quad (16)$$

The expression of $\lambda_f \widetilde{B}_{\gamma Z}(f)$ appeared already in the literature [7,12–14] as the integral representation for the Barr–Zee diagrams. In the case of top quark, and thus $N_c^t Q_t^2 I_{3t} = 2/3$ and $\lambda_t \simeq 3.6$, we expand $1/(a-\lambda_t)$ as

$$\frac{1}{a-\lambda_t} = -\frac{1}{\lambda_t} \left\{ 1 + \frac{a}{\lambda_t} + \frac{a^2}{\lambda_t^2} + \cdots \right\}, \quad (17)$$

and we obtain after the x-integration

$$N_c^t Q_t^2 I_{3t} \frac{12}{5} A_{\gamma Z}(t) = \frac{1}{\lambda_t} \left\{ \frac{2}{3} + \frac{2}{5} \log \lambda_t + \frac{1}{\lambda_t} \left[\frac{47}{375} + \frac{2}{25} \log \lambda_t \right] + \cdots \right\} + \frac{\kappa}{\lambda_t} \left\{ \frac{34}{135} + \frac{4}{9} \log \kappa \right\} + \mathcal{O}\left(\frac{\kappa}{\lambda_t^2}, \kappa^2 \right), \quad (18)$$

$$-N_c^t Q_t^2 I_{3t} \frac{12}{5} \lambda_t B_{\gamma Z}(t) = \left\{ -\frac{16}{5} - \frac{8}{5} \log \lambda_t - \frac{1}{\lambda_t} \left[\frac{4}{9} + \frac{4}{15} \log \lambda_t \right] + \cdots \right\} - \kappa \left\{ \frac{64}{45} + \frac{32}{15} \log \kappa \right\} + \mathcal{O}\left(\frac{\kappa}{\lambda_t}, \kappa^2 \right). \quad (19)$$

We see that the above equations (18) and (19) reproduce the results of the asymptotic expansion method, ΔC_Z and ΔC_G, which are given in Eqs. (9) and (10) of Ref. [7]. In addition, the subleading $\mathcal{O}(1/\lambda_t^2)$ terms and the nonleading $\mathcal{O}(\kappa)$ terms are included, respectively, in Eqs. (18) and (19), which may serve as another check on the asymptotic expansion method.

For the contribution of top quark $C_{\gamma Z}(t)$, the integral form of $8/5[\widetilde{A}_{\gamma Z}(t) - \lambda_t \widetilde{B}_{\gamma Z}(t)]$ gives -5.134 with $\lambda_t = 3.6$, while the use of the leading $\mathcal{O}(1)$ and subleading $\mathcal{O}(1/\lambda_t)$ terms in the expansions in Eqs. (18) and (19), which is the result of the asymptotic expansion method, $(\Delta C_Z + \Delta C_G)$, given in Eq. (11) of Ref. [7], leads to -5.140. Agreement is excellent and we see that the asymptotic expansion method works just fine for the case of top quark triangle loop diagrams. The integral form of $\widetilde{A}_{\gamma Z}(f)$ in Eq. (16) is still applicable to estimate $C_{\gamma Z}(f)$ for the contributions from the loops of b quark, τ lepton and c quark. Alternatively, the formula $\widetilde{A}_{\gamma Z}(f) \approx (3/2)(-2 - \ln \lambda_f)$ can be used since $\lambda_f \ll 1$ for $f = b, \tau, c$. On the other hand, for the light quarks, i.e., u, d and s quarks, there is the issue of how to properly treat their triangle loop diagrams [5,15,16]. For the contributions to a_μ from the muon and electron triangle loop diagrams, we arrive at the same formulae given by KKSS [Eqs. (4.11) and (4.12) of Ref. [4]], since $A_{\gamma Z}(f)$ in Eq. (8) is the same expression as the one derived by them.

In summary, the two-loop electroweak contributions to a_μ from fermion triangle diagrams connected to the muon line by a photon and a Z-boson depicted in Fig. 1 can be calculated without approximations. It is shown that the calculation in the unitary gauge exactly coincides with the one in the ’t Hooft–Feynman gauge. The part generated from the ordinary axial-vector Ward identity in the unitary gauge corresponds to the contribution of the neutral Goldstone boson in the ’t Hooft–Feynman gauge. For the top-quark contribution, the one-parameter integral form is obtained up to the order of m_μ^2/m_Z^2. The results are compared with those obtained by the asymptotic expansion method. We see that numerically agreement is excellent. Yet, there still remains the discrepancy of 3.3σ between experiment and theory for a_μ.

Acknowledgements

I thank T. Uematsu for reading the manuscript and for various supports. The Feynman diagrams in this paper were prepared using JaxoDraw [17].

Funding

Open Access funding: SCOAP^3.

References

[1] P. A. Zyla et al. [Particle Data Group], Prog. Theor. Exp. Phys. **2020**, 083C01 (2020).
[2] A. Czarnecki, B. Krause, and W. J. Marciano, Phys. Rev. D **52**, R2619(R) (1995).
[3] A. Czarnecki, B. Krause, and W. J. Marciano, Phys. Rev. Lett. **76**, 3267 (1996).
[4] T. V. Kukhto, E. A. Kuraev, A. Schiller, and Z. K. Silagadze, Nucl. Phys. B **371**, 567 (1992).
[5] S. Peris, M. Perrottet, and E. de Rafael, Phys. Lett. B **355**, 523 (1995).
[6] T. Ishikawa, N. Nakazawa, and Y. Yasui, Phys. Rev. D **99**, 073004 (2019).
[7] A. Czarnecki and W. J. Marciano, Phys. Rev. D **96**, 113001 (2017); **97**, 019901 (2018) [erratum].
[8] S. L. Adler, Phys. Rev. **177**, 2426 (1969).
[9] L. Rosenberg, Phys. Rev. **129**, 2786 (1963).
[10] M. E. Peskin and V. Schroeder, *An Introduction to Quantum Field Theory* (Addison-Wesley, Reading, 1995).
[11] C. Itzykson and J.-B. Zuber, *Quantum Field Theory* (McGraw-Hill, New York, 1980).
[12] S. M. Barr and A. Zee, Phys. Rev. Lett. **65**, 21 (1990); **65**, 2920 (1990) [erratum].
[13] D. Chang, W.-F. Chang, C.-H. Chou, and W.-Y. Keung, Phys. Rev. D **63**, 091301(R) (2001).
[14] K. Cheung, C.-H. Chou, and O. C. W. Kong, Phys. Rev. D **64**, 111301(R) (2001).
[15] M. Knecht, M. Perrottet, E. de Rafael and S. Peris, J. High Energy Phys. **0211**, 003 (2002).
[16] A. Czarnecki, W. J. Marciano, and A. Vainshtein, Phys. Rev. D **67**, 073006 (2003); **73**, 119901 (2006) [erratum].
[17] D. Binosi and L. Theußl, Comp. Phys. Comm. **161**, 76 (2004).